analytical chemistry

Article

pubs.acs.org/ac

Thiacalixarene Covalently Functionalized Multiwalled Carbon Nanotubes as Chemically Modified Electrode Material for Detection of Ultratrace Pb^{2+} Ions

Li Wang,*[,†] Xiaoya Wang,[†] Guosheng Shi,[‡] Cheng Peng,*[,‡] and Yihong Ding[§]

[†]Department of Chemistry, Tongji University, No. 1239 Siping Road, Shanghai 200092, China

[‡]Shanghai Institute of Applied Physics, Chinese Academy of Sciences, Shanghai 201800, China

[§]State Key Laboratory of Theoretical and Computational Chemistry, Institute of Theoretical Chemistry, Jilin University, Changchun 130023, China

ABSTRACT: This paper presents the preparation of novel thiacalixarene (TCA) covalently functionalized multiwalled carbon nanotubes (MWCNTs) and an enhanced differential pulse anodic stripping voltammetric procedure for the determination of trace amounts of Pb^{2+} ions, which relies on the selective accumulation of the metals at a TCA-MWCNT-modified glassy carbon electrode. Through a combination of thiacalixerene's excellent selective recognition and the outstanding electronic properties of MWCNTs, this electrode material shows excellent selectivity and high sensitivity for electrochemical detection of Pb^{2+} ions. The stripping response is highly linear (R = 0.999) over a Pb^{2+} concentration range of 2×10^{-10} to 1×10^{-8} mol/L, and the limit of detection is 4×10^{-11} mol/L. Furthermore, the determination of Pb^{2+} (10^{-7} mol/L) in the presence of an equal amount of interfering Sn^{2+} ions yielded well-separated signals. To understand the molecular interaction mechanism between the TCA molecules and metal ions (Pb^{2+} and Sn^{2+}), theoretical computations were performed. The results demonstrate that the Pb^{2+}/Sn^{2+} ions could stably adsorb onto the TCA molecules, and there is significant electron delocalization between Pb^{2+}/Sn^{2+} and sulfur atoms in the TCA molecule.

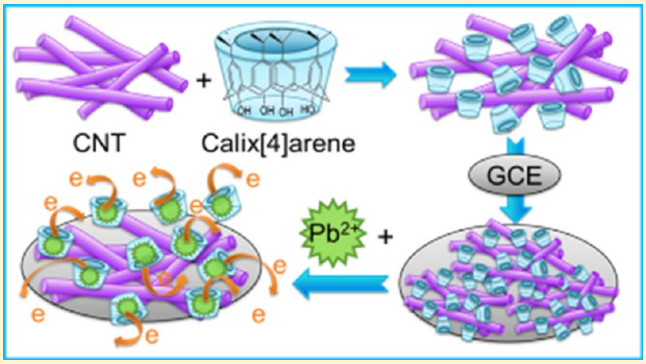

In recent years, measurements of heavy metals have been attracting increasing attention in environmental, toxicological, pharmaceutical, and biomedical analysis. New sensors and analytical procedures with better selectivity and higher sensitivity are in great demand for the quantification of trace amounts of toxic heavy metals. The electrochemical stripping method, in combination with various electrodes, is a powerful tool in trace analysis.[1−3]

Over the past few decades, the development of adsorptive stripping voltammetry has extended the scope of stripping procedures.[4] Because of the non-electrolytic accumulation of the target metal onto the surface of the working electrode, the adsorptive stripping procedure has inherent sensitivity and favorable selectivity. In addition, it has offered an alternative for stripping analysis of trace metals, which cannot be accumulated electrochemically.[5] However, ordinary electrochemical solid electrodes such as Au, Pt, glassy carbon, and graphite are not suitable for the determination of trace amounts of metal ions because of their poor sensitivity. Therefore, chemically modified electrodes (CMEs) have been introduced to improve sensitivity. The properties of the CMEs are tailored through surface modification with various selective molecular recognition elements such as selective ligands,[6,7] ion-exchange resins,[8,9] and other polymers.[10−12] Macrocyclic ligands such as crown ethers,[13−15] cyclodextrins,[16−18] and calixarenes[19−22] have been successfully used as modifiers for CMEs.

Calixarenes, known as novel molecular receptors, are attractive materials for separation and sensing applications because of their unique selective recognition ability. In electroanalysis, calixarenes were originally used at the end of the 1980s for making ion-selective electrodes[23] and more recently have been applied as electrode modifiers for voltammetric stripping analysis. However, when used as modifiers for voltammetric electrodes, calixarenes are commonly plasticized into PVC membranes[24−26] or dispersed in Nafion[27,28] coating solutions. Neither calixarenes nor these coating solutions have sufficient conductivity to produce favorable electroanalysis signals. Further, the bonding of the calixarene to the electrode is neither uniform nor stable. Therefore, a new conductive coating, in which calixarenes are uniformly incorporated by chemical bonds, is desired.

We considered carbon nanotubes (CNTs) as the new coating material because their high conductivity should offset

Received: May 24, 2012
Accepted: November 10, 2012
Published: November 11, 2012

Scheme 1. Schematic Representation of the Fabrication and Electroanalysis Mechanism of TCA/MWCNT-Modified Electrodes for Lead(II)

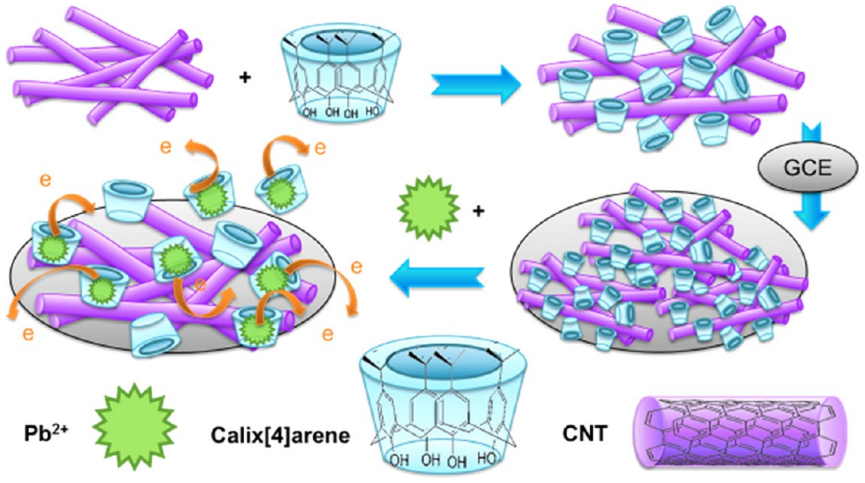

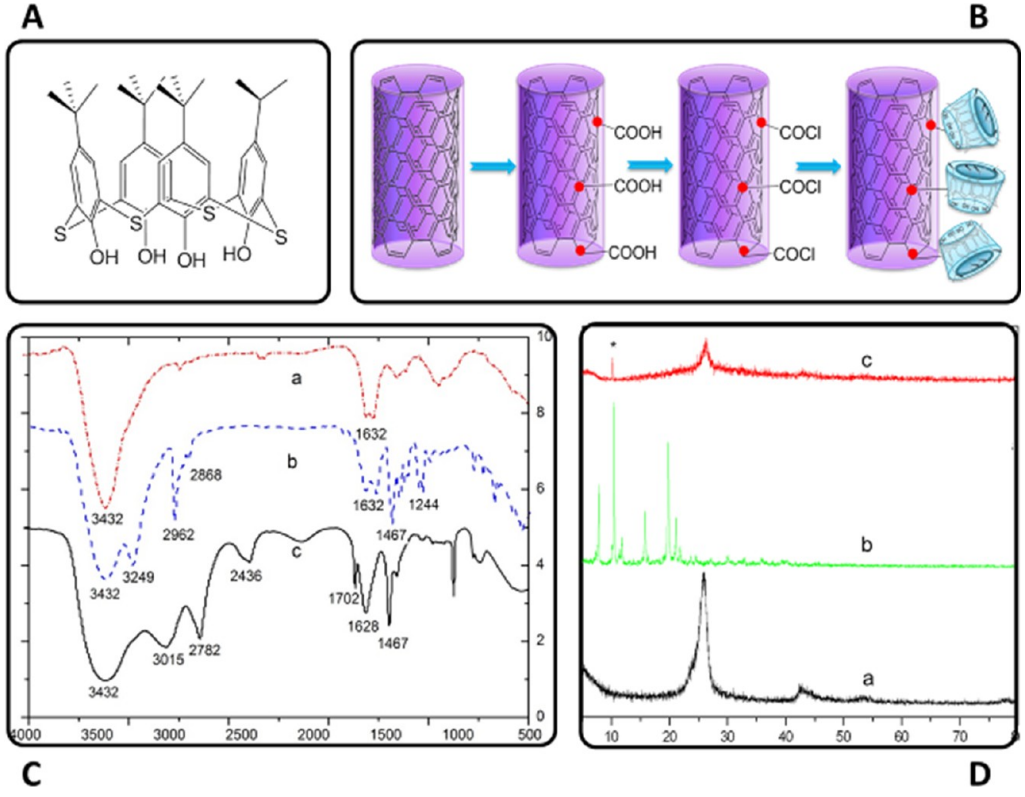

Figure 1. (A) Molecular structure of TCA. (B) Synthetic procedure for TCA-MWCNTs. (C) FTIR spectra and (D) XRD patterns of (a) MWCNTs, (b) TCA, and (c) TCA-MWCNTs.

the poor conductivity of calixarenes. CNTs are 1D nanomaterials with unique mechanical, geometric, electronic, and chemical properties,[29] which make them increasingly attractive for use in electrochemical detection. CNTs can greatly enhance electrochemical signals and thus minimize the detection limit of electrochemical devices.[30] Dramatically improved electrochemical detection has been reported for many substances such as 2,4,6-trinitrotoluene,[31] DNA,[32] dopamine,[33] and caffeine.[34] In addition, CNTs have been used to remove heavy metal ions from aqueous solutions and also to create new CMEs for determining trace amounts of heavy metals.[35−37]

However, to apply CNTs for electrochemical measurements, two problems must be solved. First, the dispersion of CNTs in most solvents is poor, owing to the strong van der Waals force between the nanotubes; this can be resolved by functionalization.[38,39] Second, CNTs do not show selective adsorption. The huge surface area and graphene sheet structure lead to strong interfacial accumulation of analyses on CNTs, without selectivity. Thereof, much effort has made on the design and preparation of nanocomposites based on CNTs that combine the high surface area and excellent conductivity of CNTs with functional organic or inorganic materials. Various types of

dx.doi.org/10.1021/ac302747f | *Anal. Chem.* 2012, 84, 10560−10567

nanocomposites based on CNTs, such as CNT−polymer and CNT-metals, have been reported.[40−44]

Herein, we have combined the excellent selectivity of calixarene with the outstanding electronic properties of CNTs by chemically bonding calixarene to CNTs. The resulting material should avoid the disadvantages of the two raw materials, while retaining their excellent properties. Electroanalytical results showed that this was indeed the case. As far as we are aware, this is the first report of combining calixarene ligands with CNTs to construct a calixarene-CNT-based CME. Scheme 1 describes the fabrication and electroanalysis mechanism of thiacalixarene (TCA)/MWCNT-modified electrodes for the detection of lead(II).

Here, we report the preparation of this new type of functional material (TCA chemically modified MWCNT) and the favorable differential pulse anodic stripping behavior of this material on glassy carbon electrodes (GCEs). In our earlier study, the TCA ligand was shown to exhibit excellent selectivity for Pb^{2+}.[45] In this work, the TCA-functionalized MCNT-modified electrode showed a highly linear response ($R = 0.999$) over a Pb^{2+} concentration range of 2×10^{-10} to 1×10^{-8} mol/L, with a very low detection limit for Pb^{2+} (4×10^{-11} mol/L). Importantly, it gave separate signals when analyzing a mixed solution containing equal amounts of Pb^{2+} ion and the interfering ion, Sn^{2+}. This behavior can be ascribed to the excellent molecular recognition ability of TCA.

MATERIALS AND METHODS

Apparatus. Differential pulse stripping voltammetric measurements were performed on an electrochemical analyzer CHI660C (CH Instrument, Shanghai) connected to a personal computer. A three-electrode configuration was employed. The working electrode was a glassy carbon disk electrode (3 mm diameter, CH Instrument) modified with TCA-MWCNTs, while Ag/AgCl and platinum wire served as the reference and counter electrodes, respectively. IR spectra were recorded on a Nicolet FT-IR NEXUS spectrometer (Thermo Scientific). X-ray diffraction was performed on a Bruker Focus D8 diffractometer. The SEM micrograph was obtained with a Hitachi S4800 scanning electron microscope (operating at 100 kV). The pH measurements were performed on a digital pH/mV meter (Cyberscan 510).

Reagents. Carbon nanotubes (MWCNT 4060), with a diameter of 40−60 nm and a length of several micrometers, were purchased from Shenzhen Nanotech Port Co., Ltd. Thiacalixarene (TCA, Figure 1A) was synthesized and characterized by means of ^{1}H NMR, IR, ESI-MS, and EA as previously reported.[45] All other chemicals were purchased commercially and of analytical grade. Solutions were prepared with doubly distilled water. Stock solutions of Pb^{2+} and Sn^{2+} were prepared from lead nitrate and tin(II) chloride dihydrate, respectively. A 0.1 M HAc-NaHAc buffer (pH 4.5) served as the supporting electrolyte in all experiments.

Synthesis of TCA-MWCNTs. Carbon nanotubes were purified prior to use by stirring in concentrated hydrochloric acid for 20 h. Then, 0.15 g of purified carbon nanotubes was added to a mixture of 4 mL of concentrated H_2SO_4 and 12 mL of concentrated HNO_3, and the suspension was stirred for 8 h at 70−80 °C, then centrifuged at 4000 rpm after cooling to room temperature. The residue was washed with 0.05 M NaOH and deionized water repeatedly until all of the acid was removed. The carboxylated product MWCNT-COOH was obtained after drying. $SOCl_2$ (20 mL) was added to MWCNT-COOH, and the mixture was stirred overnight at 70−80 °C. The unreacted $SOCl_2$ was then removed by distillation to give MWCNT-COCl. TCA (0.070 g) (excess) dissolved in 20 mL of *N*,*N*-dimethylformamide (DMF) was added directly to the obtained MWCNT-COCl, and the mixture was stirred for 24 h at 60−70 °C to produce a well-dispersed black particle suspension. The suspension was centrifuged at 4000 rpm, washed repeatedly with DMF to remove the unreacted TCA, and then washed with deionized water. The final product TCA-MWCNTs was obtained after drying.

Electrode Preparation. The GCEs were polished sequentially with 0.3, 0.1, and 0.05 μm alumina powders, then sonicated and rinsed with deionized water. TCA-MWCNTs were immobilized onto the polished GCE using acetone as the dispersing agent. The immobilizing solution was prepared by introducing 20 mg of TCA-MWCNTs into 10 mL of acetone and sonicating for 3 h to aid the dissolution of the functionalized MWCNTs. A 20 μL aliquot of this sonicated solution was cast directly onto the polished glassy carbon disk electrode using a microinjector and allowed to dry at room temperature.

Accumulation and Voltammetric Procedures. The adsorptive stripping analysis includes two steps: a non-electrochemical accumulation step at open circuit and an anodic stripping voltammetric step. For the accumulation step, the modified GCE was immersed into 30 mL of supporting electrolyte (0.1 M HAc-NaAc, pH 4.5) containing the target analyte, to allow preconcentration of the ions at open circuit potential with stirring. In most cases, a 15 min accumulation time was used. Before beginning the stripping process, the voltage was held at −0.9 V for 60 s. Then the differential pulse voltammetric (DPV) measurement was carried out from −0.9 to −0.4 V. All stripping measurements were performed in the presence of dissolved oxygen. The DPV parameters were −0.9 V deposition potential, 50 Hz frequency, 50 mV potential amplitude, and 10^{-6} A/V sensitivity.

Theoretical Computation Method. The B3LYP[46,47] method, within the generalized gradient approximation in the framework of density functional theory (DFT), is widely used to investigate interactions between metal ions and TCA.[48−50] In this work, we used this approach to examine the intermolecular interactions between the TCA and metal ions (Pb^{2+} and Sn^{2+}). For geometry optimization, we employed the 6-31G(d) basis set for carbon, hydrogen, and sulfur. In addition, a LANL2DZ pseudopotential function was introduced into the basis set for the two metal ions (Pb^{2+} and Sn^{2+}). Furthermore, the minimum energy geometries obtained from this method were recalculated using a polarizable continuum model (PCM)[51,52] to represent water, to show any additional effects of solution. All calculations were carried out using the Gaussian 09 package.[53]

RESULTS AND DISCUSSION

Synthesis and Characterization of TCA-MWCNT. The synthesis scheme is presented in Figure 1B. Purified carbon nanotubes were first oxidized by the mixture of acids and then chloroacylated by $SOCl_2$. The resulting MWCNT-COCl reacted with TCA to give TCA-MWCNTs. The final product was first characterized by Fourier transform infrared (FTIR) spectroscopy. Trace (a) in Figure 1C shows the FTIR spectrum of MWCNTs, with an absorption band at 1632 and 1467 cm^{-1} assigned to stretching vibration of the six-membered ring of carbon. The spectrum of TCA (trace b) has absorption bands

at 3249 cm^{-1} for −OH groups, 2962 and 3249 cm^{-1} for $-C(CH_3)_3$, and 1244 cm^{-1} for −Ar−S−Ar. In trace (c), the spectrum of TCA-MWCNTs, the peak at 1702 cm^{-1} is assigned to carbonyl groups (C═O stretching), which were introduced by the carboxylation of the MWCNTs; the peaks at 2782 and 3015 cm^{-1} are from the $-C(CH_3)_3$ groups in the thiacalix[4]-arene, which confirms the successful reaction of TCA with MWCNTs to form TCA-MWCNT-functionalized material. The strong absorption bands at 1632 and 1467 cm^{-1} are assigned to −Ar groups, suggesting that during the nitric acid treatment process carboxylic acid and hydroxyl groups formed mostly on the ends of the MWCNTs, without significantly damaging the MWCNT or reducing their length.

Figure 1D shows the XRD patterns of MWCNTs (a), TCA (b), and TCA-MWCNTs (c). It can be seen that the characteristic reflections of TCA are in the range of 7−23°, as shown in Figure 1D(b), and the MWCNTs exhibit a tall, narrow peak at 25.8°, as shown in Figure 1D(a). In the patterns of the final product (trace c), a reflection characteristic of TCA can be observed at 10°, while the CNT peak appeared at 26.2° and became much shorter and broader compared with that in trace (a). The attachment of the TCA groups to the surfaces of the MWCNTs caused a shift in the CNT peak by about 0.4°, which reveals that its crystalline state has changed. The change in peak shape indicates that the crystallinity of the MWCNTs has decreased greatly because the functionalization of the CNTs at their ends, defect sites, and along their sidewalls has weakened the interactions between carbon atoms in the MWCNTs, and because of the steric issue, they just cannot pack in as ordered a way as they used to before TCA groups were added. These XRD patterns are evidence that the TCA has covalently bound to the MWCNTs.

Figure 2 shows the SEM images of layers of MWCNTs (A) and TCA-MWCNTS (B) cast on the GCE surface. Both SEM images show that the GCE surfaces are coated with relatively homogeneous MWCNT films. Furthermore, the morphologies of MWCNTs were well retained after modification, which indicated that the characteristics of MWCNTs, such as high electron conductivity and large surface area, were well retained.

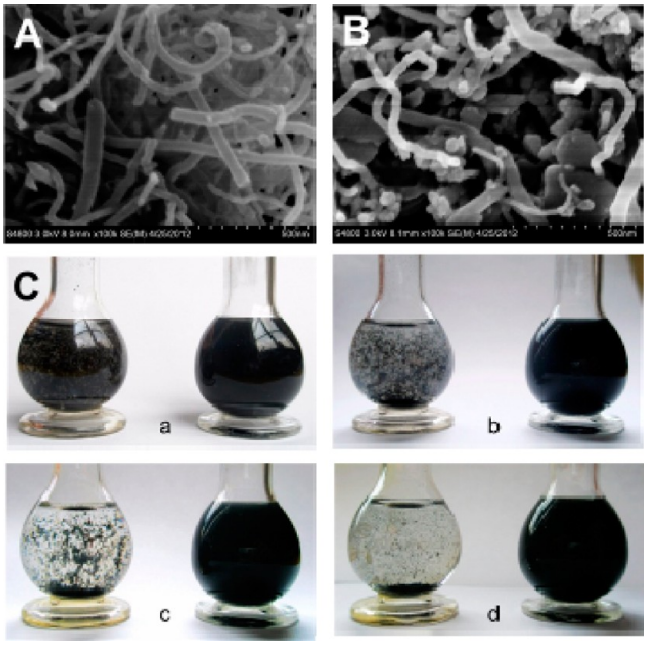

Figure 2. SEM images of (A) MWCNTs and (B) TCA-MWCNTs cast on the electrode surface, and (C) photographs of MWCNTs (left bottle) and TCA-MWCNTs (right bottle) dispersed in acetone, after standing for (a) 1 h, (b) 8 h, (c) 1 day, and (d) 1 week.

In summary, the IR spectra and XRD patterns indicate that the TCA has indeed been chemically bound to the surface of the CNTs. SEM images illustrate that the morphologies of MWCNTs were retained after the attachment of the TCA groups.

Dispersion. The following experiments were performed to investigate the dispersion of the TCA-MWCNT material. MWCNTs (20 mg) or the equivalent TCA-MWCNTs were added to 10 mL bottles of acetone and sonicated for 3 h. Both samples became homogeneous black suspensions. Figure 2C shows images of the two suspensions after standing for particular times.

It is obvious that the MWCNTs in the left-hand bottle aggregated and tended to settle within an hour. After 8 h, settling of this sample is complete. In contrast, the TCA-MWCNT dispersed in the right-hand bottle remained homogeneous and almost retained the same appearance throughout the standing time. This shows that the dispersion of TCA-MWCNTs is much better than that of unmodified MWCNTs, and this result is consistent with the decrease of the crystallinity of the TCA-MWCNTs, as mentioned above.

Stability of Electrode Modification. MWCNTs and TCA-MWCNTs were used as electrode modifiers for fabrication of CMEs. Before any detection was performed using these CMEs, the current−time (i−t) curve method was used to show that the modified layer on the surface of the GC electrode stayed in place. In an amperometric i−t curve, a constant potential is applied and the current is recorded as a function of time. Current fluctuation would be caused by any tiny changes in the solution or on the electrode. Figure 3A shows i−t curves for both electrodes measured in supporting electrolyte containing 10^{-7} M Pb^{2+}. Both electrodes exhibited a rapid increase in current initially and before reaching a steady state. The period required to reach the maximum steady-state current was very short, which suggests low diffusion resistance and high electronic conductivity for both electrodes. After holding at constant potential for 5 min, both curves were very smooth without fluctuations, indicating that the modified electrodes were stable and that the modifiers had not detached.

Stripping Voltammetric Measurements of Pb^{2+}. Modification of GCEs with a TCA-MWCNT layer contributes to strong accumulation of Pb^{2+} from the solution phase onto the surface of the modified electrode under open circuit conditions. Figure 3B shows the DPV curves obtained from a 1×10^{-7} M Pb^{2+} solution after 15 min accumulation using the bare GCE, MWCNT-modified GCE, and TCA-MWCNT-modified GCE. The three GCEs showed very different sensitivities. The response on the bare GCE was almost not detectable (curve a). With identical conditions, the TCA-free MWCNT-modified GCE (curve b) gave a signal at −0.525 V because of the absorbing effect of the MWCNTs, while a remarkable increase in response signal was observed on the TCA-functionalized MWCNT-modified GCE (curve c). This clearly demonstrates the favorable signal-enhancing effect of the TCA-MWCNTs.

Scheme 2 illustrates the proposed mechanism of the stripping voltammetric measurement. First, (a) Pb^{2+} ions were accumulated from the solution phase onto the surface of the CME by selective complexation with the ligand (TCA) at

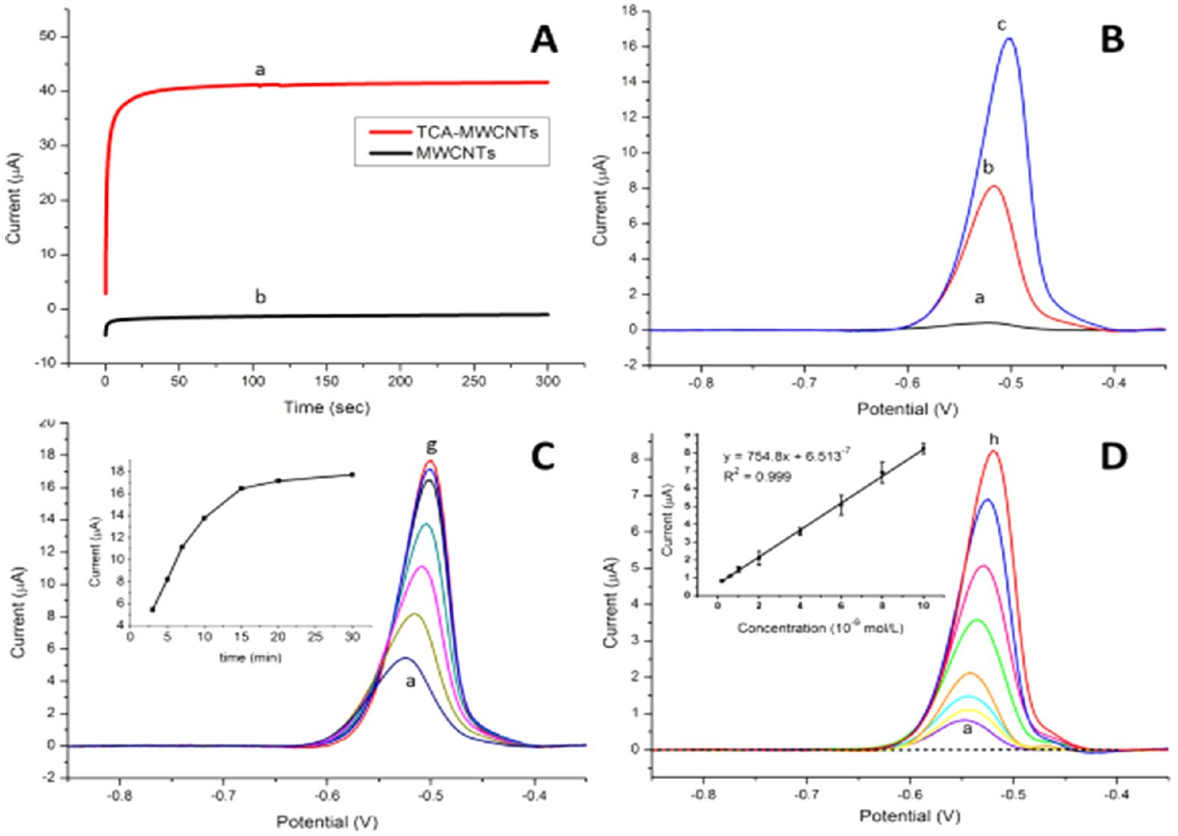

Figure 3. (A) Current−time (i−t) curves of (a) TCA-MWCNT-modified electrode and (b) MWCNT-modified electrode. (B) Differential pulse anodic stripping voltammetric (DPASV) response signals from 10^{-7} M Pb^{2+} solutions, after 15 min accumulation using different GCEs: (a) bare GCE, (b) MWCNT/GCE, and (c) TCA-MWCNT/GCE. (C) DPASV responses of 10^{-7} M Pb^{2+} using a TCA-MWCNT/GCE after 3, 5, 7, 10, 15, 20, and 30 min accumulation times (curves a−g). (D) DPASV responses at the TCA-MWCNT/GCE after 15 min accumulation with increasing levels of Pb^{2+} from 2×10^{-10} to 1×10^{-8} M (the concentrations of Pb^{2+} from curves a to h are 2×10^{-10}, 5×10^{-10}, 1×10^{-9}, 2×10^{-9}, 4×10^{-9}, 6×10^{-9}, 8×10^{-9}, and 1×10^{-8} M, respectively), along with the response to the blank solution (dotted line). Conditions for i−t curve: initial E = −0.9 V, sampling interval = 0.1 s, run time = 300 s, sensitivity (A/V) = 10^{-4}. DPV conditions: scan from −0.9 V to −0.3 V, amplitude = 0.05 V, pulse width = 0.05 s, sample width = 0.0167 s, pulse period = 0.2 s, sensitivity = $1e^{-5}$A/V.

Scheme 2. Proposed Accumulation and Voltammetric Mechanism

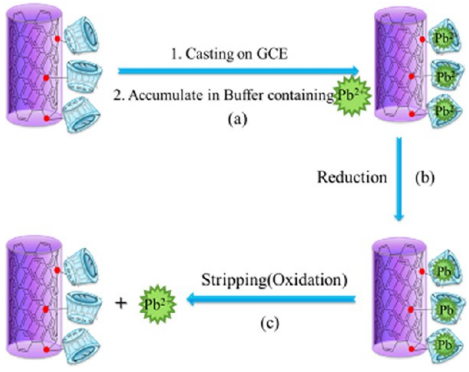

open circuit conditions, and then (b) the Pb^{2+} ions accumulated in the modifying layer were reduced to Pb^0 by applying a constant voltage of −0.9 V. Finally, lead is electrochemically stripped back into the solution by scanning toward positive potential using the DPV method (c). Thus the accumulation time should be the length of time required for the complexation reaction between TCA molecules and Pb^{2+} ions, and the resulting stripping peak should be proportional to the amount of Pb^{2+} ions in the solution being tested.

The effect of accumulation time was investigated at constant Pb^{2+} concentration (10^{-7} M) for times between 3 and 30 min. Figure 3C shows that the increase of the stripping signal with accumulation time was rapid initially and then reached a plateau; for accumulation times of at least 15 min, the stripping signals remained almost constant. This indicates that 15 min is sufficient for the complexation reaction between TCA and Pb^{2+} ions. Therefore, 15 min was selected as the accumulation time for subsequent experiments.

Well-defined response signals were obtained for different Pb^{2+} concentrations after 15 min accumulation, and these favorable response characteristics offer convenient quantification of low parts per billion levels of lead ions (Figure 3D). The calibration plot based on the peak heights of the stripping signals was found to be linear in the concentration range from 2×10^{-10} to 1×10^{-8} M ($y = 754.8x + 6.513^{-7}$). The limit of detection of the method was calculated to be 4×10^{-11} M. To the best of our knowledge, this is the lowest detection limit reported to date and is probably attributable to the extraordinary recognition ability of the TCA ligand and the excellent electronic properties of the MWCNTs in this new type of material.

Interferences. Because of the molecular recognition ability of the TCA ligand, our modified electrode was expected to exhibit excellent selectivity toward lead(II) in the presence of

different interfering ions. To verify this expectation, adsorptive stripping voltammetry was carried out by spiking a 0.1 mM Pb^{2+} containing solution with Zn^{2+}, Cd^{2+}, and Ni^{2+} ions in 100-fold excess compared with the lead concentration, and the results are shown in Figure 4A. Detection of Pb^{2+} was clearly

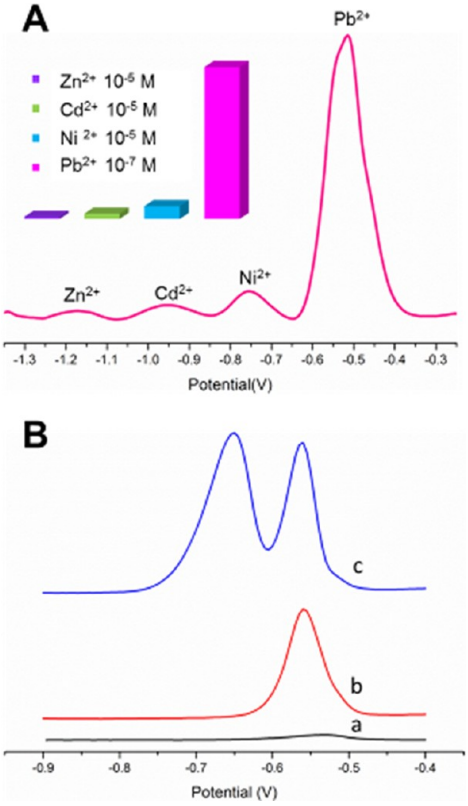

Figure 4. DPASV response signals after 15 min accumulation of (A) 10^{-7} M Pb^{2+} containing 100-fold excess amounts of Zn^{2+}, Ni^{2+}, and Cd^{2+} ions and (B) 10^{-7} M Pb^{2+} containing 10^{-7} M Sn^{2+} at different GCE: (a) bare GCE, (b) MWCNT/GCE, and (c) TCA-MWCNT/GCE. DPV conditions here are the same as in Figure 3.

not affected by Zn^{2+}, Cd^{2+}, or Ni^{2+}, showing that the modified electrode is able to exploit the excellent selective recognition of the thiacalix[4]arene ligand toward Pb^{2+}, as was previously found.[54]

The most surprising result of these selectivity studies was the performance of the electrode in the presence of Sn^{2+}. In most electrolytes, the peak potentials of Sn^{2+} and Pb^{2+} are so close together that voltammetric determination is impossible. The determination of lead by voltammetric methods in the presence of tin is difficult because of the overlapping stripping peaks.[55,56] Therefore, Sn^{2+} ions are the most important interference in the analogous anodic stripping voltammetry measurement of Pb^{2+}.[57] To study the interference effect of Sn^{2+} on the determination of Pb^{2+}, differently modified electrodes were tested with a 10^{-7} M Pb^{2+} solution containing the same amount of Sn^{2+} ions.

Figure 4B shows the differential pulse anodic stripping voltammetric (DPVSV) signals. With a MWCNT-modified GCE, no new peak appeared with the addition of tin(II), which means that both the signals of lead(II) and tin(II) were completely overlapped at −0.55 V because of the strong adsorption property and poor selectivity of CNTs. In contrast, with the TCA-MWCNT-modified GCE, a new peak at −0.65 V (shifted by nearly 0.1 V) was recorded, which did not interfere with the original peak. The TCA-MWCNT-modified GCE enabled us to separate the signals of Pb^{2+} and Sn^{2+}, which can be attributed to the complexation between TCA and Pb^{2+} ions or Sn^{2+} ions.

Molecular Interaction Mechanism. To further understand the mechanism of molecular interaction between the TCA molecule and metal ions (Pb^{2+} and Sn^{2+}), we performed the theoretical calculation at the B3LYP method in the framework of the density functional theory (DFT). The most stable structure of TCA is shown in Figure 5A. Figure 5B−I

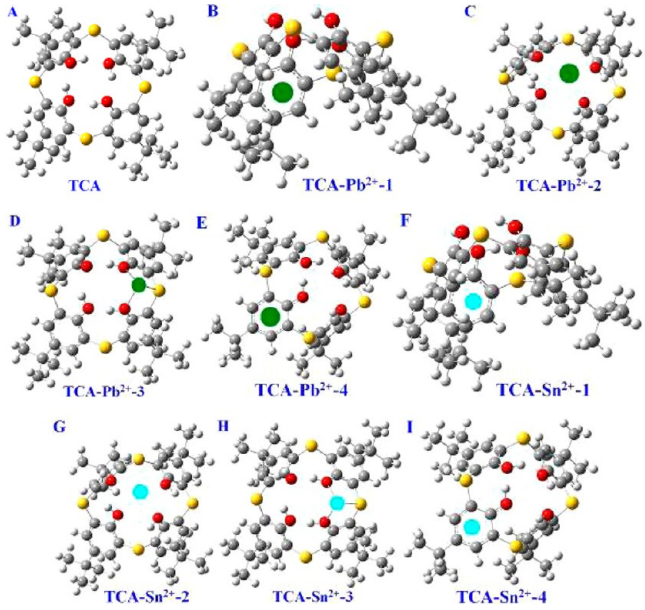

Figure 5. (A) Most stable structure of the TCA molecule was obtained at the B3LYP/6-31G(d) level. (B−I) Possible structures of the TCA-metal ion complexes (Pb^{2+} and Sn^{2+}) were obtained using the B3LYP method combined with the 6-31G(d) basis set for oxygen, carbon, sulfur, and hydrogen atoms and LANLl2DZ basis set for metal ions (Pb^{2+} and Sn^{2+}). The TCA and metal ions are shown with carbon in gray, hydrogen in white, oxygen in red, sulfur in orange, lead in green, and tin in cyan.

shows possible geometric configurations of the TCA-metal ion complexes (Pb^{2+} and Sn^{2+}). From them, we learned that there were four different bonding positions for adsorption of metal ions (Pb^{2+} and Sn^{2+}) onto the TCA molecule. Pb^{2+} and Sn^{2+} ions could adsorb onto the aromatic rings inside (see Figure 5B,F) or outside (see Figure 5E,I) the TCA molecules via cation−π interactions. Figure 5C,G shows that the Pb^{2+} and Sn^{2+} ions could be adsorbed between four hydroxyl groups. Figure 5D,H shows that the Pb^{2+} and Sn^{2+} ions could complex with two oxygen atoms and one sulfur atom, respectively. Next, we considered the strength of the adsorption of the Pb^{2+} and Sn^{2+} ions onto a TCA molecule via computation of the adsorption energies. The adsorption energies of Pb^{2+} and Sn^{2+} ions on a TCA molecule (ΔE_i) were defined as

$$\Delta E_i = E_{TCA\text{-}i} - E_{TCA} - E_i$$

where $E_{TCA\text{-}i}$, E_{TCA}, and E_i are the total energies of the metal ions adsorbed on the TCA molecule, a TCA molecule, and the metal ions, respectively. The adsorption energies are shown in Table 1. From Table 1, we can see that the most stable structures of the Pb^{2+}/Sn^{2+}-TCA compounds were TCA-Pb^{2+}/

dx.doi.org/10.1021/ac302747f | Anal. Chem. 2012, 84, 10560−10567

Table 1. Adsorption energies (ΔE_i) for different sites determined using the B3LYP method combined with the 6-31G(d) basis set for oxygen, carbon, sulfur and hydrogen atoms and LANL2DZ basis set for metal ions (Pb^{2+} and Sn^{2+})

TCA-metal compounds	ΔE_i (kcal/mol)
TCA-Pb^{2+}-1	−168.4
TCA-Pb^{2+}-2	−173.3
TCA-Pb^{2+}-3	−188.8
TCA-Pb^{2+}-4	−131.9
TCA-Sn^{2+}-1	−171.4
TCA-Sn^{2+}-2	−188.2
TCA-Sn^{2+}-3	−209.9
TCA-Sn^{2+}-4	−148.1

Sn^{2+}-3 (see Figure 5D,H). The adsorption energies of TCA-Pb^{2+}-3 and TCA-Sn^{2+}-3 were −188.8 and −209.9 kcal/mol, respectively, which demonstrates that the Pb^{2+}/Sn^{2+} ions could stably adsorb onto the TCA molecules in the gas state. We then performed single-point calculations at this method with a polarizable continuum model (PCM in water for the most stable structures, TCA-Pb^{2+}-3 and TCA-Sn^{2+}-3) to show the solution effect. The adsorption energies of TCA-Pb^{2+}-3 and TCA-Sn^{2+}-3 were −22.2 and −42.7 kcal/mol in the water solution, which are more than 3 times that of a hydrogen bond (~6 kcal/mol) and 37 k_BT for T = 300 K, indicating that both Pb^{2+} and Sn^{2+} ions are still stably adsorbed onto the TCA molecule when it is in water. Our results also showed a difference of about 20.5 kcal/mol between the adsorption energies of TCA-Pb^{2+}-3 and TCA-Sn^{2+}-3 in the water. This shows that complexation with TCA separates the peak potentials of lead and tin ions and allows the determination of tin ions and lead ions in mixtures by voltammetric methods.

Analysis of the molecular orbitals was performed to further understand the Pb^{2+}/Sn^{2+}-TCA interaction mechanism. Two unoccupied molecular orbitals, LUMO and LUMO+1, of the Pb^{2+}/Sn^{2+}-TCA compounds were plotted, as shown in Figure 6. They are representative of all molecular orbitals involved in the interactions between Pb^{2+}/Sn^{2+} and TCA. Figure 6A,C shows the partial electron delocalization between Pb^{2+}/Sn^{2+} and oxygen atoms in the TCA molecule, and Figure 6B,D shows the partial electron delocalization between Pb^{2+}/Sn^{2+} and sulfur atoms in the TCA molecule. These figures clearly show that the delocalized electrons occupy regions between the Pb^{2+}/Sn^{2+} ions and the TCA molecule when they are adsorbed on the TCA molecule, indicating an good electric conduction between the adsorbed Pb^{2+}/Sn^{2+} ions and the TCA molecule.

Determination of Lead in Water Sample. The method developed was applied for determination of lead in Tongxin river water (Table 2). Each sample was prepared by filtering the water sample through filter paper and then diluting 100 μL of a water sample 100-fold with supporting electrolyte.

Table 2. Determination of Lead in River Water Samples[a]

sample	added (nmol/L)	found (nmol/L)	recovery (%)
river water		2.23 (±0.23)	
	1.00	3.26 (±0.05)	103.0
	2.00	4.24 (±0.22)	100.5

[a]Values in parentheses are standard deviations of three replicate measurements.

The analysis was performed by the procedure described above, using a standard addition method to eliminate the effect of the matrix. The good recoveries show the practical applicability of our new electrode.

CONCLUSIONS

We report the synthesis of a new type of material, TCA-MWCNTs, and the use of an electrode modified with this material in a sensitive voltammetric method for detection of ultratrace Pb^{2+} ions. Because our electrode material combines the excellent selectivity of calixarene and the outstanding electrical conductivity and high surface area of MWCNTs, we obtain excellent selectivity and extremely high sensitivity, allowing convenient quantification of Pb^{2+} down to sub-microgram/liter level with a LOD of 4×10^{-11} mol/L. Determination of Pb^{2+} (1×10^{-7} M) in the presence of an equal amount of Sn^{2+}, which is usually an interfering ion, yielded well-separated signals. Theoretical computation showed that Pb^{2+}/Sn^{2+} ions could stably adsorb onto the TCA molecules, and that there was significant electronic conduction between the adsorbed Pb^{2+}/Sn^{2+} ions and the TCA molecule. Complexation with TCA allows us to quantify tin ions or lead ions by voltammetric methods in the presence of the other ions.

AUTHOR INFORMATION

Corresponding Author

*E-mail: wangli@tongji.edu.cn, pengcheng@sinap.ac.cn.

Notes

The authors declare no competing financial interest.

ACKNOWLEDGMENTS

We thank Prof. Chunhai Fan, Prof. Qing Huang, and Prof. Haiping Fang for their help. The authors thank the National Natural Science Foundation of China for support of this research (Grant Nos. 51102272, 31170776, 21073074,

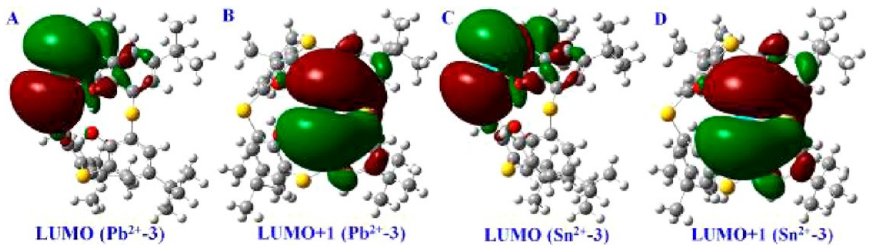

Figure 6. LUMO and LUMO+1 of the Pb^{2+}/Sn^{2+}-TCA compounds. The TCA and metal ions are shown with carbon in gray, hydrogen in white, oxygen in red, sulfur in orange, lead in green, and tin in cyan. The electron density is plotted for iso-values of ±0.01 au, with red and green denoting regions of opposite signs.

20773054, and 10825520). Moreover, this work was supported by the National Basic Research Program of China (973 Program) (Nos. 2007CB936000, 2012CB932800, and 2012CB932400), the Doctor Foundation of the Ministry of Education (No. 20070183028), the Excellent Young Teacher Foundation of the Ministry of Education of China, the Excellent Young People Foundation of Jilin Province (No. 20050103), the Program for New Century Excellent Talents in University (NCET), and the Shanghai Supercomputer Center of China.

REFERENCES

(1) He, S. J.; Li, D.; Zhu, C. F.; Song, S. P.; Wang, L. H.; Long, Y. T.; Fan, C. H. *Chem. Commun.* **2008**, 4885−4887.
(2) Zhu, Z. Q.; Su, Y. Y.; Li, J.; Li, D.; Zhang, J.; Song, S. P.; Zhao, Y.; Li, G. X.; Fan, C. H. *Anal. Chem.* **2009**, *81*, 7660−7666.
(3) Guo, S. J.; Li, J.; Ren, W.; Wen, D.; Dong, S. J.; Wang, E. K. *Chem. Mater.* **2009**, *21*, 2247−2257.
(4) Brett, C. M. A.; Oliveira Brett, A. M. C. F.; Pereira, J. L. C. *Electroanalysis* **1991**, *3*, 683−689.
(5) Arrigan, D. W. M. *Analyst* **1994**, *119*, 1953−1966.
(6) Burshtain, D.; Mandler, D. *ChemPhysChem* **2004**, *5*, 1532−1539.
(7) Gadhari, N. S.; Sanghavi, B. J.; Srivastava, A. K. *Anal. Chim. Acta* **2011**, *703*, 31−40.
(8) Ghodbane, O.; Roue, L.; Belanger, D. *Chem. Mater.* **2008**, *20*, 3495−3504.
(9) Singh, A. V.; Sharma, N. K. *Water SA* **2011**, *37*, 295−302.
(10) Gholivand, M. B.; Azadbakht, A.; Pashabadi, A. *Electroanalysis* **2011**, *23*, 364−370.
(11) Buica, G. O.; Ungureanu, E. M.; Birzan, L.; Razus, A. C.; Bujduveanu, M. R. *Electrochim. Acta* **2011**, *56*, 5028−5036.
(12) Wen, Y. L.; Pei, H.; Wan, Y.; Su, Y.; Huang, Q.; Song, S. P.; Fan, C. H. *Anal. Chem.* **2011**, *83*, 7418−7423.
(13) Agrahari, S. K.; Kumar, S. D.; Srivastava, A. K. *J. AOAC Int.* **2009**, *92*, 241−247.
(14) Kotkar, R. M.; Desai, P. B.; Srivastava, A. K. *Sens. Actuators, B* **2007**, *124*, 90−98.
(15) Kotkar, R. M.; Srivastava, A. K. *Sens. Actuators, B* **2006**, *119*, 524−530.
(16) Hromadova, M.; Sokolova, R. *Curr. Org. Chem.* **2011**, *15*, 2950−2956.
(17) Tredici, I.; Merli, D.; Zavarise, F.; Profumo, A. *J. Electroanal. Chem.* **2010**, *645*, 22−27.
(18) Frasconi, M.; Mazzei, F. *Nanotechnology* **2009**, 20.
(19) Cadogan, F.; Kane, P.; McKervey, M. A.; Diamond, D. *Anal. Chem.* **1999**, *71*, 5544−5550.
(20) Mokhtari, B.; Pourabdollah, K.; Dalali, N. *J. Inclusion Phenom. Macrocyclic Chem.* **2011**, *69*, 1−55.
(21) Giannetto, M.; Mori, G.; Notti, A.; Pappalardo, S.; Parisi, M. F. *Chem.—Eur. J.* **2001**, *7*, 3354−3362.
(22) El Nashar, R. M.; Wagdy, H. A. A.; Aboul-Enein, H. Y. *Curr. Anal. Chem.* **2009**, *5*, 249−270.
(23) Diamond, D.; Svehla, G.; Seward, E. M.; McKervey, M. A. *Anal. Chim. Acta* **1988**, *204*, 223−231.
(24) Tyagi, S.; Agarwal, H.; Ikram, S. *Water Sci. Technol.* **2010**, *61*, 693−704.
(25) Shamsipur, M.; Beigi, A. A. M.; Teymouri, M.; Rasoolipour, S.; Asfari, Z. *Anal. Chem.* **2009**, *81*, 6789−6796.
(26) Gupta, V. K.; Jain, A. K.; Al Khayat, M.; Bhargava, S. K.; Raisoni, J. R. *Electrochim. Acta* **2008**, *53*, 5409−5414.
(27) Torma, F.; Gruen, A.; Bitter, I.; Toth, K. *Electroanalysis* **2009**, *21*, 1961−1969.
(28) Ramkumar, J.; Maiti, B. *Sens. Actuators, B* **2003**, *96*, 527−532.
(29) Iijima, S. *Nature* **1991**, *354*, 56−58.
(30) Yuan, W.; Che, J. F.; Chan-Park, M. B. *Chem. Mater.* **2011**, *23*, 4149−4157.
(31) Wang, J.; Hocevar, S. B.; Ogorevc, B. *Electrochem. Commun.* **2004**, *6*, 176−179.
(32) Luque, G. L.; Ferreyra, N. F.; Granero, A.; Bollo, S.; Rivas, G. A. *Electrochim. Acta* **2011**, *56*, 9121−9126.
(33) Baldrich, E.; Gomez, R.; Gabriel, G.; Munoz, F. X. *Biosens. Bioelectron.* **2011**, *26*, 1876−1882.
(34) Zhang, J.; Wang, L. P.; Guo, W.; Peng, X. D.; Li, M.; Yuan, Z. B. *Int. J. Electrochem. Sci.* **2011**, *6*, 997−1006.
(35) Guo, X. F.; Yun, Y. H.; Shanov, V. N.; Halsall, H. B.; Heineman, W. R. *Electroanalysis* **2011**, *23*, 1252−1259.
(36) Tofighy, M. A.; Mohammadi, T. *J. Hazard. Mater.* **2011**, *185*, 140−147.
(37) Morton, J.; Havens, N.; Mugweru, A.; Wanekaya, A. K. *Electroanalysis* **2009**, *21*, 1597−1603.
(38) Eitan, A.; Jiang, K. Y.; Dukes, D.; Andrews, R.; Schadler, L. S. *Chem. Mater.* **2003**, *15*, 3198−3201.
(39) Chattopadhyay, J.; de Jesus Cortez, F.; Chakraborty, S.; Slater, N. K. H.; Billups, W. E. *Chem. Mater.* **2006**, *18*, 5864−5868.
(40) Saleh, F. S.; Rahman, M. R.; Kitamura, F.; Okajima, T.; Mao, L. Q.; Ohsaka, T. *Electroanalysis* **2011**, *23*, 409−416.
(41) Pan, D.; Wang, Y.; Chen, Z.; Yin, T.; Qin, W. *Electroanalysis* **2009**, *21*, 944−952.
(42) Huang, S. Q.; Li, L.; Yang, Z. B.; Zhang, L. L.; Saiyin, H.; Chen, T.; Peng, H. S. *Adv. Mater.* **2011**, *23*, 4707−4710.
(43) Giambastiani, G.; Cicchi, S.; Giannasi, A.; Luconi, L.; Rossin, A.; Mercuri, F.; Bianchini, C.; Brandi, A.; Melucci, M.; Ghini, G.; Stagnaro, P.; Conzatti, L.; Passaglia, E.; Zoppi, M.; Montini, T.; Fornasiero, P. *Chem. Mater.* **2011**, *23*, 1923−1938.
(44) Chen, W. F.; Wu, J. S.; Kuo, P. L. *Chem. Mater.* **2008**, *20*, 5756−5767.
(45) Hu, X. J.; Pan, Z. G.; Wang, L.; Shi, X. F. *Spectrochim. Acta, Part A* **2003**, *59*, 2419−2423.
(46) Becke, A. D. *Phys. Rev. A* **1988**, *88*, 3098.
(47) Lee, C.; Yang, W.; Parr, R. G. *Phys. Rev. B* **1988**, *37*, 785.
(48) Yang, K.; Kang, K. D.; Park, Y. H.; Koo, I. S.; Lee, I. *Chem. Phys. Lett.* **2003**, *381*, 239−243.
(49) Zheng, X.; Wang, X.; Yi, S.; Wang, N.; Peng, Y. J. *Comput. Chem.* **2010**, *31*, 1458−1468.
(50) Xia, Y.; Wang, X.; Zhang, Y.; Luo, B. *Comput. Theor. Chem.* **2011**, *967*, 235−242.
(51) Cammi, R.; Mennucci, B.; Tomasi, J. *J. Phys. Chem. A* **2000**, *104*, 5631−5637.
(52) Cossi, M.; Scalmani, G.; Rega, N.; Barone, V. *J. Chem. Phys. Lett.* **2002**, *117*, 43.
(53) Frisch, M. J.; Trucks, G. W.; Schlegel, H. B.; Scuseria, G. E.; Robb, M. A.; Cheeseman, J. R.; Scalmani, G.; Barone, V.; Mennucci, B.; Petersson, G. A.; Nakatsuji, H.; Caricato, M.; Li, X.; Hratchian, H. P.; Izmaylov, A. F.; Bloino, J.; Zheng, G.; Sonnenberg, J. L.; Hada, M.; Ehara, M.; Toyota, K.; Fukuda, R.; Hasegawa, J.; Ishida, M.; Nakajima, T.; Honda, Y.; Kitao, O.; Nakai, H.; Vreven, T.; Montgomery, J. A., Jr.; Peralta, J. E.; Ogliaro, F.; Bearpark, M.; Heyd, J. J.; Brothers, E.; Kudin, K. N.; Staroverov, V. N.; Kobayashi, R.; Normand, J.; Raghavachari, K.; Rendell, A.; Burant, J. C.; Iyengar, S. S.; Tomasi, J.; Cossi, M.; Rega, N.; Millam, N. J.; Klene, M.; Knox, J. E.; Cross, J. B.; Bakken, V.; Adamo, C.; Jaramillo, J.; Gomperts, R.; Stratmann, R. E.; Yazyev, O.; Austin, A. J.; Cammi, R.; Pomelli, C.; Ochterski, J. W.; Martin, R. L.; Morokuma, K.; Zakrzewski, V. G.; Voth, G. A.; Salvador, P.; Dannenberg, J. J.; Dapprich, S.; Daniels, A. D.; Farkas, Ö.; Foresman, J. B.; Ortiz, J. V.; Cioslowski, J.; Fox, D. J. *Gaussian 09*, revision A.1; Gaussian, Inc.: Wallingford, CT, 2009.
(54) Wang, L.; Li, H. H.; Jiang, Z. L.; Gu, J. Y.; Shi, X. F. *J. Inclusion Phenom. Macrocyclic Chem.* **2002**, *42*, 39−43.
(55) Lin, L.; Thongngamdee, S.; Wang, J.; Lin, Y.; Sadik, O. A.; Ly, S. *Anal. Chim. Acta* **2005**, *535*, 9−13.
(56) Dong, S.; Wang, Y. *Anal. Chim. Acta* **1988**, *212*, 341−347.
(57) Dirilgen, N.; Dogan, F. *Int. J. Environ. Anal. Chem.* **2004**, *84*, 855−864.